Validation campaigns for Aeolus with the ALADIN Airborne Demonstrator and 2-µm Doppler wind lidar team

Christian Lemmerz (a), Benjamin Witschas (a), Oliver Lux (a), Stephan Rahm (a), Karsten Schmidt (b), Uwe Marksteiner (a), Alexander Geiß (c), Andreas Schäfler (a), Fabian Weiler (a) and Oliver Reitebuch (a)

(a) Deutsches Zentrum für Luft- und Raumfahrt e.V., DLR, Institute für Physik der Atmosphäre, Oberpfaffenhofen 82234, Germany

(b) Deutsches Zentrum für Luft- und Raumfahrt (DLR), Institut für Methodik der Fernerkundung, Oberpfaffenhofen 82234, Germany

(c) Ludwig-Maximilians-University Munich, Meteorological Institute, 80333 Munich, Germany

christian.lemmerz@dlr.de

Abstract: The German Aerospace Center (DLR) has conducted four airborne campaigns with a focus on validating the Aeolus wind products during different states of the ESA mission since launch in 2018. During these campaigns, the DLR Falcon aircraft was equipped with the ALADIN Airborne Demonstrator (A2D), which is the prototype of the direct-detection wind lidar instrument on-board Aeolus, together with a high-accuracy scanning coherent-detection 2-µm Doppler wind lidar (DWL), used as a reference. Complementary and synergistic results from both DWLs allow for characterizing the Aeolus wind errors and to provide recommendations for the optimization of the Aeolus wind retrieval.

Keywords: Aeolus, space-borne wind lidar, coherent wind lidar, direct-detection wind lidar, validation.

1. Introduction

The ESA Aeolus mission is the first spaceborne Doppler wind lidar and provides profiles of the wind vector component along the instrument's line-of-sight (LOS) direction from ground up to about 30 km in the stratosphere [1]. After launch on 22 August 2018, Aeolus was injected into a sun-synchronous dusk-dawn orbit at about 320 km altitude. Its single payload is the Atmospheric Laser Doppler Instrument (ALADIN), a direct-detection wind lidar operating at an ultraviolet wavelength of 354.8 nm and designed to determine the Doppler shift of the backscattered light from both molecules and particles and hence the LOS wind speed. The backscattered light collected by a 1.5 m diameter telescope is first directed to a Fizeau interferometer to analyze the frequency shift of the narrowband particulate (Mie) return signal from detecting the position of a transmitted fringe imaged on an accumulating charge coupled device (ACCD) detector. Most of the light is rejected by the Fizeau and reflected to two sequentially coupled Fabry–Pérot interferometers. Their transmission functions are separated in frequency such that the Doppler shift of the broadband molecular (Rayleigh) return signal is determined by comparing the individual transmitted intensities, both detected with a second ACCD. Range bins can be set for a vertical resolution between 250 m and 2 km and changed along the orbit. The complex optical arrangement has proven its ability to capture the wind fields along the orbit already three weeks after launch. In the following years, the Aeolus data assimilation has also demonstrated to improve numerical weather prediction (NWP) with remarkable impact especially in the medium-range weather forecast [2], even at the degraded signal performance observed in mid-2022.

A significant contribution to this quick and impressive mission success was the experience gained during the mission preparation phase through various pre-launch activities with the A2D, which was developed based on the Aeolus instrument ALADIN pre-development receiver optics and electronics [3] to maximize technological representativity in design and measurement principle. The A2D allowed to verify and validate the complex direct-detection measurement technique for wind and aerosol, its operational limits, instrument calibration procedures, alignment sensitivity, noise characteristics and many more specifics of the instrument. This knowledge was consequently used to test and refine the processors developed well ahead of the mission phase. The validation was performed by ground and

airborne measurements often paired with a coherent-detection reference wind lidar (2-µm DWL) providing a high sensitivity to particulate returns and the ability to measure accurate wind vector profiles [4]. Thus, these activities had demonstrated the capabilities expected for Aeolus already before launch and continued during the mission phase. For the airborne activities the two DWLs were installed onboard the DLR Falcon research aircraft to capture wind profiles from an altitude of 10 km to 11 km down to the ground along the Aeolus measurement track. More than 26,000 km of collocated measurements along the Aeolus track were recorded during four airborne campaigns in different geographical regions and under diverse atmospheric and solar background conditions, while covering different Aeolus performance phases. The following sections describe the airborne campaigns and their results in determining the Aeolus L2B wind product's systematic and random errors as well as potential improvements of the wind retrieval algorithms.

2. DLR Aeolus Validation Campaigns Overview

Based on the experience of the pre-launch campaigns including WindVal [5] and WindVal-II [6] around Iceland in 2015 and 2016, respectively, DLR conducted the first Aeolus airborne validation campaign WindVal-III already during the commissioning phase in late 2018. From the base in Oberpfaffenhofen, Germany four flights were conducted along ascending orbits in the evening hours. This campaign was followed by a second campaign in central Europe, also conducted from Oberpfaffenhofen, which started the series of validation campaigns during the operational phase of the Aeolus mission. AVATAR-E (Aeolus Validation Through Airborne Lidars in Europe) was covering six underflights again on ascending orbits, but in the late phase of the active period of the Aeolus laser A with decreased lidar signal performance in spring of 2019. In autumn of the same year, after the laser B had been commissioned, the artic and North Atlantic region was targeted from a base in Keflavík, Iceland during the AVATAR-I campaign. The total of ten underflights also included, for the first time, four flights on descending orbits that were performed in the early morning hours, as well as flights along the high albedo snow-covered east coast of Greenland. A main focus lied also in capturing the strong wind speeds and gradients associated with the polar jet stream in the region. This was supported by a dedicated range bin setting (RBS) for Aeolus, allowing higher vertical resolution in the campaign area. Delayed by more than one year due to COVID-19 related logistic issues, the tropical region was the scene for the AVATAR-T campaign in autumn of 2021.

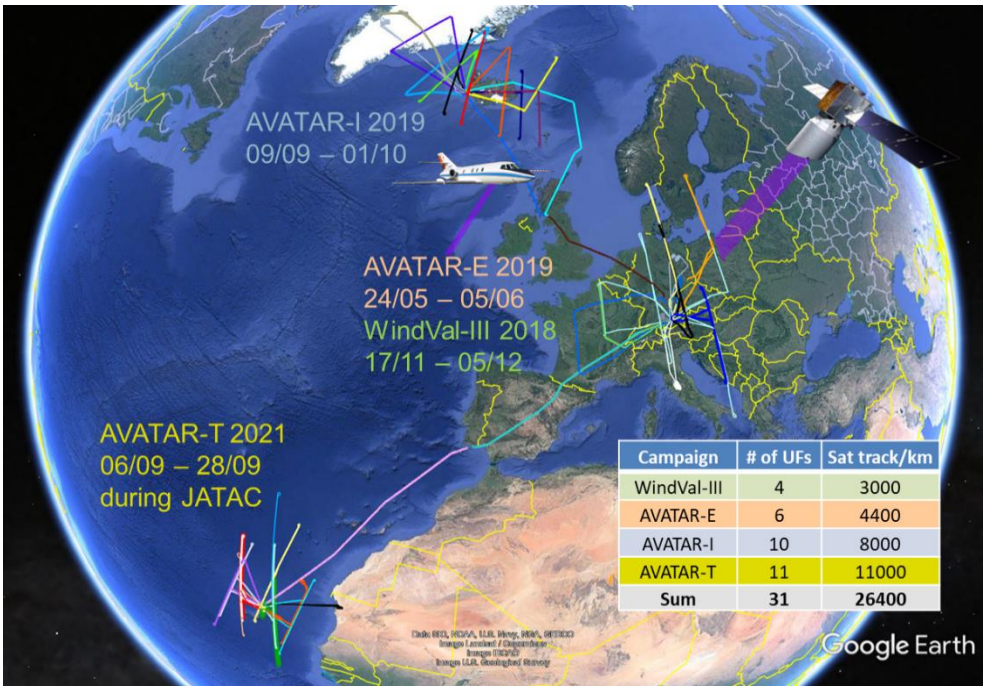

Campaign	# of UFs	Sat track/km
WindVal-III	4	3000
AVATAR-E	6	4400
AVATAR-I	10	8000
AVATAR-T	11	11000
Sum	**31**	**26400**

Figure 1. Overview of the four DLR airborne campaigns with their flight tracks performed for the Aeolus validation in different mission phases and locations. The insert table summarizes the campaign statistics with the number of satellite underflights (UFs).

Five descending and six ascending orbit underflights were conducted with a focus on the specific atmospheric conditions influenced by strong Saharan dust outbreaks and the African Easterly Jet (AEJ) winds around the Cape Verdean Archipelago. With a base in Sal this campaign was embedded in the Joint Aeolus Tropical Atlantic Campaign (JATAC) together with ESA, NASA, CNES/LATMOS and other partners. JATAC was carried out with contributions from the DC-8, the German and French Falcons and a strong ground-based and light aircraft component organized by NOA and TROPOS, offering a wide range of in-situ as well as active and passive remote sensing measurement equipment [7]. A dedicated RBS was active in the region during the JATAC focusing on high resolution in the middle troposphere. During all campaigns, additional calibration flights were conducted for the A2D where the aircraft is rolled 20° to the right and circles an area, while the lidar is pointing nadir to justify the assumption of zero wind influence on the LOS during the performed frequency sweep to characterize the spectrometer responses [5]. An overview of all campaign flights is given in Figure 1 together with a table of the campaign statistics.

3. Results

Individual flights as well as whole campaign datasets provide an intermediate validation perspective between the local validation by ground sites and the more global perspective of NWP-based validation strategies. Collocated airborne measurements also ensure a high representativity with a time difference to the overpass of usually not more than 45 minutes. For Aeolus this allows for studying the influence of different atmospheric scenes on the performance of the Mie and Rayleigh channel wind products in terms of coverage and error distribution. As an example, results from an around 900 km long flight leg performed along an ascending orbit during the AVATAR-T campaign are shown in Figure 2. As the Aeolus L2B Rayleigh-clear and Mie-cloudy products as well as the ECMWF model background winds are provided for the horizontal LOS (HLOS), for comparison also the airborne lidar wind measurements have to be transferred to the wind speed nomenclature (positive winds blowing away from the instrument) and horizontal component of the Aeolus viewing direction. Figure 2 shows the finer resolution for the measured airborne data in the left column, which provides insights into errors in the Aeolus data products stemming from vertical or horizontal inhomogeneities. For the statistical comparison, the airborne data is averaged to the coarser vertical and horizontal resolution of the Aeolus measurement grid. The procedures applied for the statistical comparison with the airborne DWL data and results of the systematic and random errors in both Aeolus channels are described in detail by Witschas et al. [4] and Lux et al. [8] for the first two campaigns, as well as in the contribution by Witschas et al. [9] for the CLRC 2022 for the two later campaigns.

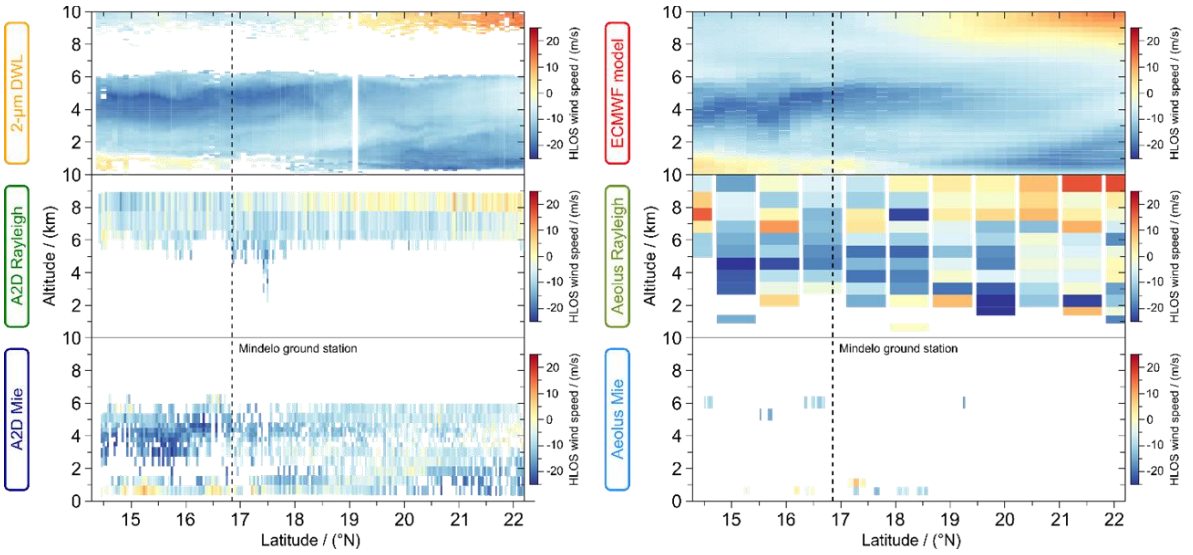

Figure 2. Example of the wind data products for an Aeolus validation flight on Friday, 10 September 2021 also passing the ground measurement site in Mindelo. 2-µm measurements and the ECMWF model winds are shown in the upper row with Rayleigh and Mie channel winds measured by the A2D (left) and Aeolus (right) below, all shown for the HLOS wind component.

The best Aeolus performance was observed in the frame of the AVATAR-I campaign which took place during the early laser B period in autumn 2019. Here, comparison of the Aeolus winds against 2-µm DWL data yielded random errors (in terms of the scaled median absolute deviation) of 3.8 m/s for Rayleigh-clear winds during ascending orbits, and 2.3 m/s for the Mie-cloudy winds during descending orbits, respectively. Both values were obtained after averaging to a vertical bin thickness of 1 km.

Focusing on the wind data of the 2-µm DWL in Figure 2, it is clear that the signal coverage of the coherent system is limited to the first 1 km below the aircraft and the dust-laden Saharan Air Layer (SAL). Within the SAL detailed structures of the AEJ are revealed with horizontal wind speeds of up to 20 m/s, while the ECMWF model winds partly show deficiencies in correctly representing the AEJ position and strength. The A2D Rayleigh winds provide good coverage in the aerosol-free regions, while the Mie channel covers the winds within the SAL and down to the surface. The importance of the winds in clear atmosphere and the abundance of aerosol-free regions in weather-relevant altitudes around the globe were the main drivers to justify the UV wavelength and spectrometer arrangement of Aeolus, and thus the design of the A2D (although the Mie channel has a lower sensitivity compared to the very sensitive coherent detection). This is especially obvious when comparing the covered regions of A2D and Aeolus Rayleigh and Mie channels. The Aeolus Mie-cloudy product only provides very few valid wind results, as the processors are not optimized for the strong aerosol scattering case within the SAL, which is still lower than cloud return signals. A2D results suggest that a refinement of the Aeolus processor detection limits could lead to enabling a "Mie-aerosol" wind product as well as to a more effective rejection of detrimental particulate return signals that affect the Rayleigh-clear winds. The quality of Rayleigh winds detected in these altitude regions is currently decreased by both this so-called channel cross-talk and the signal attenuation within the SAL. The same is true for winds that are measured within and/or below similar layers of aerosol or thin clouds around the globe.

4. Outlook

The campaign data acquired during the four DLR airborne campaigns with the 2-µm and A2D DWLs will be further exploited to characterize the Aeolus L2B wind products, to improve the error assessment and quality control schemes as well as to support the refinement of the processors. Campaign data has already been and will be used to validate the quality of reprocessed data. Correlative analysis with the various atmospheric data from multiple instruments available from the tropical campaign partners is planned to be performed within the JATAC community. The successful approach has been to understand and validate the Aeolus-specific issues, first by comparing the 2-µm and A2D results, before transferring the knowledge to the coarser Aeolus products in a second step. This will remain to be relevant for the ongoing analysis of the campaign data as well as for the evaluation of future processor updates and re-processed data for the whole mission, well beyond the foreseeable de-orbiting of Aeolus in 2023.

5. References

[1] European Space Agency (ESA), "ADM-Aeolus Science Report", ESA SP-1311, 121 p., https://earth.esa.int/documents/10174/1590943/AEOL002.pdf, (2008).

[2] M. P. Rennie, L. Isaksen, F. Weiler, J. Kloe, T. Kanitz, O. Reitebuch, "The impact of Aeolus wind retrievals in ECMWF global weather forecasts", Q. J. R. Meteorol. Soc., https://doi.org/10.1002/qj.4142, (2021)

[3] O. Reitebuch, C. Lemmerz, E. Nagel, U. Paffrath, Y. Durand, M. Endemann, F. Fabre, M. Chaloupy, "The Airborne Demonstrator for the Direct-Detection Doppler Wind Lidar ALADIN on ADM-Aeolus. Part I: Instrument Design and Comparison to Satellite Instrument", J. Atmos. Oceanic Technol., 26, 2501–2515, https://doi.org/10.1175/2009JTECHA1309.1, (2009).

[4] B. Witschas, C. Lemmerz, A. Geiß, A., O. Lux, U. Marksteiner, S. Rahm, O. Reitebuch, F. Weiler, "First validation of Aeolus wind observations by airborne Doppler wind lidar measurements, Atmos. Meas. Tech., 13, 2381–2396 (2020).

[5] U. Marksteiner, C. Lemmerz, O. Lux, S. Rahm, A. Schäfler, B. Witschas, O. Reitebuch, "Calibrations and Wind Observations of an Airborne Direct-Detection Wind LiDAR Supporting ESA's Aeolus Mission", Remote Sensing, 10, 2056, (2018).

[6] O. Lux, C. Lemmerz, F. Weiler, U. Marksteiner, B. Witschas, S. Rahm, A. Schäfler, O. Reitebuch, "Airborne wind lidar observations over the North Atlantic in 2016 for the pre-launch validation of the satellite mission Aeolus", Atmos. Meas. Tech., 11, 3297–3322, (2018).

[7] G. Skofronick-Jackson, T. Fehr, D. Althausen, V. Amiridis, H. Baars, et al., "The Joint Aeolus Tropical Atlantic Campaign - First Results for Aeolus Calibration/Validation and Science in the Tropics", ATMOS 2021, ESA (2021).

[8] O. Lux, C. Lemmerz, F. Weiler, U. Marksteiner, B. Witschas, S. Rahm, A. Geiß, O. Reitebuch, "Intercomparison of wind observations from the European Space Agency's Aeolus satellite mission and the ALADIN Airborne Demonstrator", Atmos. Meas. Tech., 13, 2075–2097 (2020).

[9] B. Witschas, A. Geiß, O. Lux, C. Lemmerz, U. Marksteiner, A. Schäfler, S. Rahm, O. Reitebuch, F. Weiler, "Validation of the Aeolus L2B wind product by means of airborne wind lidar measurements performed in the North Atlantic region and in the tropics", extended abstract submitted to CLRC 2022, (2022).